Journal of Hydrology 472–473 (2012) 355–366

Contents lists available at SciVerse ScienceDirect

Journal of Hydrology

journal homepage: www.elsevier.com/locate/jhydrol

Regionalization and spatial changing properties of droughts across the Pearl River basin, China

Qiang Zhang [a,b,c,*], Mingzhong Xiao [a,b,c], Vijay P. Singh [d,e], Jianfeng Li [a,b,c]

[a] Department of Water Resources and Environment, Sun Yat-sen University, Guangzhou 510275, China
[b] Key Laboratory of Water Cycle and Water Security in Southern China of Guangdong High Education Institute, Sun Yat-sen University, Guangzhou 510275, China
[c] School of Geography and Planning, Guangdong Key Laboratory for Urbanization and Geo-simulation, Sun Yat-sen University, Guangzhou 510275, China
[d] Department of Biological and Agricultural Engineering, Texas A&M University, College Station, TX 77843-2117, USA
[e] Department of Civil and Environmental Engineering, Texas A&M University, College Station, TX 77843-2117, USA

ARTICLE INFO

Article history:
Received 17 February 2012
Received in revised form 15 August 2012
Accepted 30 September 2012
Available online 10 October 2012
This manuscript was handled by Andras Bardossy, Editor-in-Chief, with the assistance of Ercan Kahya, Associate Editor

Keywords:
Regionalization of droughts
Multivariate homogeneity test
Multivariate regional frequency analysis
Pearl River basin

SUMMARY

In frequency analysis for droughts, the absence of lengthy records usually limits the reliability of statistical estimates. To overcome this limitation, a "regional" analysis approach is often used. Hydrological events typically have multivariate characteristics; therefore it is logical to jointly consider these characteristics when carrying out a multivariate regional frequency analysis for these events. This study presents a method for regional frequency analysis in the Pearl River basin using the multivariate L-moments homogeneity test. Results indicate that the Pearl River basin can be categorized into five homogeneous regions in terms of drought variation, and the Plackett copula fits well for all of the homogeneous regions. The frequency analysis of all sites in each homogeneous region shows that the Pearl River Delta is characterized by a high drought risk, while a relatively lower drought risk in the west and northeast parts of the Pearl River basin. Results of this study will be useful for basin-scale water resources management across the Pearl River basin.

1. Introduction

A drought is a period dominated by abnormally dry weather that lasts long enough to produce a serious imbalance in the water cycle. Droughts have strong social and economic impacts, and can have a devastating effect on agriculture, water supply, energy, ecosystem, and the economy, causing deleterious impacts on the society. It is estimated that the global economic losses caused by droughts are as high as 6–8 billion US dollars each year, being far more than other meteorological disasters (Wilhite, 2000). However, in recent decades, due to the population growth and expansion of agricultural, energy and industrial sectors, the demand for water resources has increased manyfold and even water scarcity has been occurring almost every year in many parts of the world (Mishra and Singh, 2010). Other factors, such as climate change and contamination of water supplies, have further contributed to water scarcity (e.g. Vörösmarty et al., 2000). Drought is perceived as one of the most expensive and least understood natural disasters (e.g. Kao and Govindaraju, 2010). Therefore, increasing attention is being given in recent years to analyze changing properties, causes, impacts and evaluation of the risk of droughts (e.g. Zou et al., 2005; Livada and Assimakopoulos, 2007; Zhang et al., 2009a; Cancelliere and Salas, 2010; Lei and Duan, 2011; Liu et al., 2011; Lloyd-Hughes, 2012).

So far, no widely-accepted definition of a drought is available due to the wide variety of factors affecting droughts and also limited knowledge about them. The widely-used classification of droughts was proposed by Dracup et al. (1980). Wilhite and Glantz (1985) grouped droughts into four categories: meteorological, agricultural, hydrologic, and socioeconomic. Generally, water deficits related to precipitation, soil moisture, and streamflow are considered as meteorological, agricultural, and hydrologic droughts, respectively. Socioeconomic droughts are usually associated with the supply and demand of certain economic goods (Shiau and Shen, 2001). This study focuses on the meteorological drought.

In stochastic analysis for droughts, such as frequency analysis, the absence of lengthy records usually limits the reliability of statistical estimates. To circumvent this limitation, "regional" analysis approach is often used. For regionalization, a homogeneity test was proposed by Hosking and Wallis (1993). Yang et al. (2010) analyzed precipitation extremes using this homogeneity test in the Pearl River basin. However, it should be noted that hydrometeorological events are usually complex and are often characterized by the joint behavior of several random variables, which are not

* Corresponding author at: Department of Water Resources and Environment, Sun Yat-sen University, Guangzhou 510275, China.
E-mail address: zhangq68@mail.sysu.edu.cn (Q. Zhang).

0022-1694/$ - see front matter © 2012 Elsevier B.V. All rights reserved.
http://dx.doi.org/10.1016/j.jhydrol.2012.09.054

usually independent, such as storm duration and intensity; flood peak, volume and duration; and drought severity, duration and magnitude. These multivariate features of floods, storms or droughts are crucial for engineering planning, design, and management activities. Therefore, Chebana and Ouarda (2007) further developed the discordancy statistic and the homogeneity test proposed by Hosking and Wallis (1993) for multivariate cases. A multivariate version of L-moments, defined by Serfling and Xiao (2007), was used in this study to develop the multivariate discordancy and homogeneity statistics, and multivariate hydrological events from the Pearl River basin were modeled using a copula function.

The objectives of this study therefore are: (1) to regionalize the Pearl River basin for identifying different spatial changing properties of droughts in different parts of the river basin; and (2) analyzing the drought characteristics of each homogeneous region using a copula function.

2. Study region and data

2.1. Description of the Pearl River basin

The Pearl River basin is a humid region with abundant precipitation. However, recent years have witnessed serious droughts with high drought intensity and many prolonged water deficit periods, such as the severe drought in southwest China in 2010 and south China in 2011. Increasingly frequent droughts in recent years have inflicted devastating impacts on regional socio-economic development and eco-environment in the Pearl River basin. Besides, water shortages induced by water pollution have further deteriorated water resources availability in the Pearl River basin. Moreover, some tributaries of the Pearl River basin bear the heavy responsibility of water supply for the mega-cities in the vicinity of the Pearl River Delta. The East River, one of the major tributaries of the Pearl River basin, is utilized to satisfy the primary annual water demand of major cities, such as Hong Kong, Guangzhou, Shenzhen, Dongguan and Huizhou, with over forty million dwellers (Yang et al., 2010), and more than 80% of Hong Kong's annual water demand is satisfied by the water supply from the East River (Wong et al., 2010). Considering the significance of water security in the Pearl River basin, an improved understanding of the statistical behavior of droughts is of paramount importance to formulating a regional water resources management strategy.

2.2. Basin characteristics and data

The Pearl River (102°14′E–115°53′E; 21°31′N–26°49′N) (Fig. 1) is the second largest river in terms of water volume and the third largest river in terms of drainage basin area in China. The Pearl River basin is 4.573×10^5 km^2 in drainage area with three major tributaries: the West River, the North River and the East River. The Pearl River basin is located in the tropical and sub-tropical climate zones with annual mean temperature ranging from 14 °C to 22 °C and long-term annual average precipitation of 1525.1 mm. Precipitation during April–September accounts for 80% of the annual total. In this study, daily precipitation data covering January 1st, 1960–December 31st, 2005, was collected from 42 rain gauging stations in the Pearl River basin. Locations of the rain gauging stations are shown in Fig. 1. There were a few missing data in the daily precipitation dataset. Of the 42 stations, 7 stations had some missing data but in total the missing data was less than 0.01%. The missing precipitation data were filled in by the average value of its neighboring days. It was considered that the gap filling method would have little influence on the long-term temporal trend. Furthermore, the data consistency was checked by the double-mass method and it was found that all the data series used in the study were consistent (Zhang et al., 2009b).

3. Methodology

Multivariate regional frequency analysis method has been used to analyze the spatial changing properties of droughts in the Pearl River basin, the procedure is illustrated in Fig. 2, and the details of these methods used for the multivariate regional frequency analysis are introduced as follows.

3.1. Standardized Precipitation Index (SPI)

McKee et al. (1993) proposed SPI for the evaluation of drought conditions in Colorado. The SPI can consider the precipitation conditions in a desired period in a long-term record, and then reflect the precipitation deficits of the corresponding period in different years. As it can be calculated for a variety of time scales to monitor short-term water supplies and long-term water resources, the SPI has been widely used for studying different aspects of droughts (Guttman, 1999; Shiau, 2006; Livada and Assimakopoulos, 2007; Zhang et al., 2009a). The SPI computation is based on the long-term precipitation record for a desired time scale. This long-term record is fitted to a probability distribution, which is then transformed to a standard normal distribution (McKee et al., 1993). Given the precipitation series of a precipitation station, moving average monthly precipitation series is calculated at k time scales (e.g. $k = 3$, 6, 12, 24 months) based on the original precipitation series. As significant auto-correlation may exist in the precipitation series, to resolve this issue, the precipitation is further grouped into 12 subsets by its ending months (such as January, February,..., December), then, gamma probability density functions are fitted to these subsets for a specified time scales. Finally the SPI value is calculated by transforming the cumulative probabilities of the Gamma distribution to the standard normal distribution (McKee et al., 1993; Kao and Govindaraju, 2010). In this study, the time scale of SPI was selected as 6 months, just as the time scales of dry and wet alterations in the Pearl River basin.

3.2. Theory of runs

The theory of runs, proposed by Yevjevich (1967), was used to identify drought's characteristics (Fig. 3). A run is defined as a portion of the time series of a drought variable, in which all values are either below or above the selected truncation level. For classification of droughts (Table 1), the truncation level was held as −0.99 in the run analysis, as when the SPI is below −0.99, it is classified as drought. The drought duration was the period when SPI was continuously below the truncation level and drought severity was the cumulative deficit below the truncation level for the duration of the drought event. Then two important properties, drought duration and severity, were analyzed for each drought event.

3.3. Multivariate L-moments

Multivariate L-moments were developed by Serfling and Xiao (2007). Let $X(j)$ be a random variable with distribution F_j, for $j = 1, 2$. By analogy with a covariance representation of L-moments of order $k \geqslant 1$, multivariate L-moments are matrices Λ_k with L-comoment elements defined by:

$$\lambda_{k[ij]} = Cov\left(X^{(i)}, P^*_{k-1}\left(F_j(X^{j})\right)\right) \quad i,j = 1,2 \text{ and } k = 2,3,\ldots \tag{1}$$

where P^*_k is the so-called shifted Legendre polynomial. Note that elements $\lambda_{k[ij]}$ and $\lambda_{k[ji]}$ are not necessarily equal. Particularly, the first L-comoment elements are:

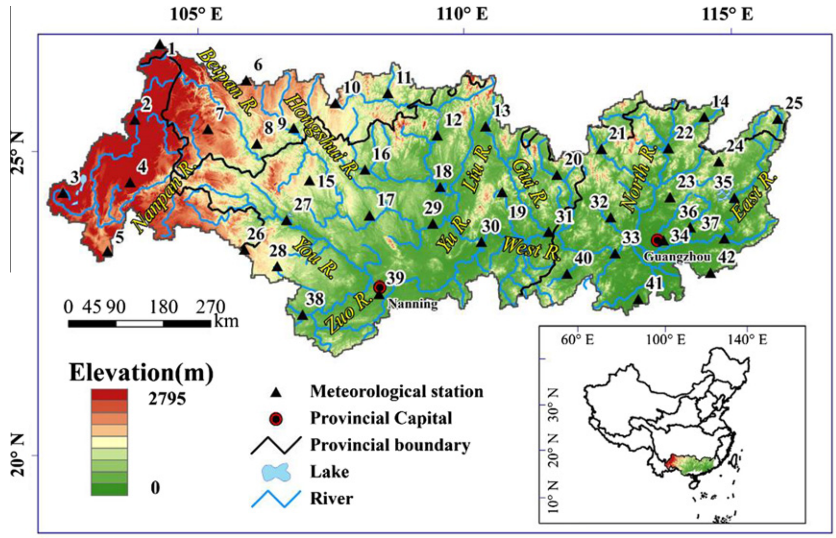

Fig. 1. Study region and meteorological stations.

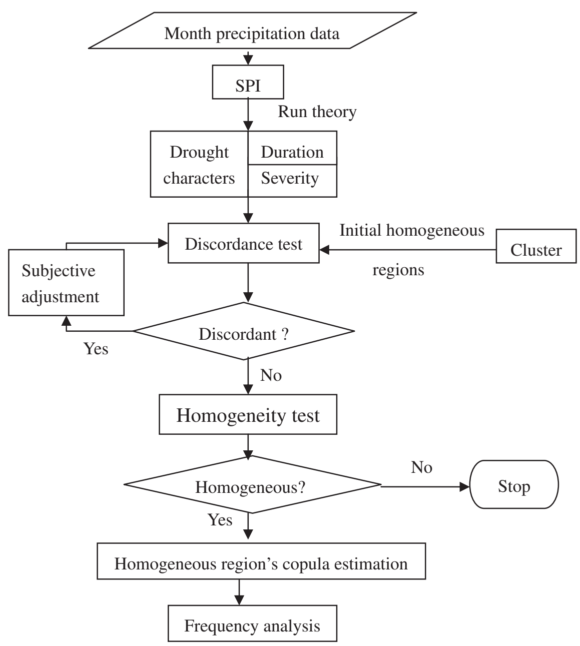

Fig. 2. Flowchart that illustrates the procedure of multivariate regional frequency analysis.

$$\lambda_{2[12]} = 2Cov\left(X^{(1)}, F_2\left(X^{(2)}\right)\right) \tag{2}$$

$$\lambda_{3[12]} = 6Cov\left(X^{(1)}, \left(F_2(X^{(2)}) - 1/2\right)^2\right) \tag{3}$$

$$\lambda_{4[12]} = Cov(X^{(1)}, 20(F_2(X^{(2)}) - 1/2)^3 - 3((F_2(X^{(2)}) - 1/2) + 1)) \tag{4}$$

which are, respectively, the L-covariance, L-coskewness and L-cokurtosis. The L-comoment coefficients are given by:

$$\tau_{k[12]} = \frac{\lambda_{k[12]}}{\lambda_2^1}, \quad k \geqslant 3 \text{ and } \tau_{2[12]} = \frac{\lambda_{2[12]}}{\lambda_1^1} \tag{5}$$

where $\lambda_k^{(j)} = \lambda_{k[jj]}$ is the classical kth L-moment of the variable $X(j)$, $j = 1,2$, as defined by Hosking (1990). A hierarchy of intuitively appealing analogs of the classical covariance and the central comoments was thus provided by L-comoments. Their interpretation and comparison are facilitated by their definition in terms of the classical covariance operator. The matrix of the L-comoment coefficients is written as (Chebana and Ouarda, 2007):

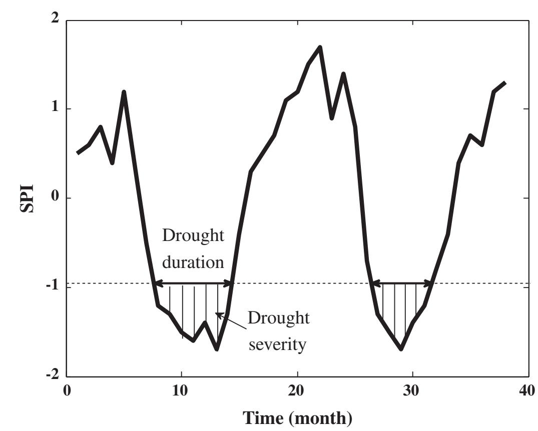

Fig. 3. Definition of drought events using runs theory.

Table 1
Drought categories based on Standardized Precipitation Index (SPI).

Category	SPI
Extremely wet	⩾2.00
Severely wet	1.50–1.99
Moderately wet	1.00–1.49
Near normal	−0.99 to 0.99
Moderate drought	−1.00 to −1.49
Severe drought	−2.00 to −1.50
Extreme drought	⩽−2.00

$$\Lambda_k^* = \left(\tau_{k[ij]}\right)_{i,j=1,2} = \begin{pmatrix} \tau_{k[11]} & \tau_{k[12]} \\ \tau_{k[21]} & \tau_{k[22]} \end{pmatrix} \tag{6}$$

Particularly, for $k = 2$ the L-covariance matrix is given by:

$$\Lambda_2^* = \begin{pmatrix} \tau_{2[11]} & \tau_{2[12]} \\ \tau_{2[21]} & \tau_{2[22]} \end{pmatrix} \tag{7}$$

According to Chebana and Ouarda (2007), the L-comoments are similar in structure and behavior to the univariate L-moments and capture their attractive properties. The multivariate L-moments defined previously are based on a theoretical population distribution; however their finite sample versions are useful to define statistical tests and also to estimate multivariate distribution parameters, as presented by Serfling and Xiao (2007). Computation was conducted based on the R software package 'lmomco' by Asquith et al. (2011), who proposed an implementation of these finite sample L-comoments.

3.4. Copulas

Since copulas model the dependence structure between random variables, irrespective of the type of marginals involved, they have recently been receiving increasing attention in various areas (e.g. Nelsen, 2006). More particularly, the copula method is being used in describing the statistical behavior of hydro-meteorological extremes (e.g., Zhang and Singh, 2006; Zhang et al., 2011). The development of copulas theory can be found in Nelsen (2006). A copula is a function C: $I \times I \to I$ ($I = [0,1]$) such that:

- for all u, $v \in I$: $C(u,0) = 0$, $C(u,1) = u$, $C(0,v) = 0$, and $C(1,v) = v$;
- for all u_1, u_2, v_1, $v_2 \in I$ such that $u_1 \leqslant u_2$ and $v_1 \leqslant v_2$:

$$C(u_2, v_2) - C(u_2, v_1) - C(u_1, v_2) + C(u_1, v_1) \geqslant 0 \tag{8}$$

Sklar (1959) advocated that the most general marginal-free description of the dependence structure of multivariate distributions is through its copula. Let F and G denote the marginal distribution functions of random variables x and y, and let H be a joint distribution function with F and G. Then, there exists a copula C such that for all real x and y,

$$H(x,y) = C(F(x), G(y)) \tag{9}$$

There are many copula families and Archimedean, Extreme Value and Plackett copulas represent classes of particular interest in hydrology (Kao and Govindaraju, 2008; Zhang and Singh, 2007; Renard and Lang, 2007).

3.4.1. Bivariate Archimedean copulas

A bivariate Archimedean copula is characterized by a generator $\phi(\cdot)$, that is a convex decreasing function satisfying $\phi(1) = 0$ where:

$$C(u,v) = \phi^{-1}(\phi(u) + \phi(v)), \quad 0 < u, v < 1 \tag{10}$$

3.4.2. Bivariate extreme value copulas

An extreme value copula is defined as

$$C(u,v) = \exp\left\{(\log u + \log v)A\left(\frac{\log u}{\log u + \log v}\right)\right\}, \quad 0 < u, v < 1 \tag{11}$$

where A is a convex function defined on $[0,1]$ with $\max(t, 1-t) \leqslant A(t) \leqslant 1$. A simple and popular copula is the Gumbel–Hougaard copula:

$$C_m(x,y) = \exp\{-[(-\log x)^m + (-\log y)^m]^{1/m}\} \tag{12}$$

where $m \geqslant 1, 0 \leqslant x, y \leqslant 1$. The Gumbel–Hougaard copula is the only one that can simultaneously satisfy the conditions of the extreme-value copula and the Archimedean copulas.

3.4.3. Bivariate Plackett copulas (Kao and Govindaraju, 2008)

The Plackett family of bivariate distributions (Plackett, 1965) was proposed based on the theory of constant crossproduct ratio (or odds ratio). For a given (u, v), the crossproduct ratio ψ_{UV} at the bivariate level can be defined as

$$\psi_{UV} = \frac{P[U \leqslant u, V \leqslant v]P[U > u, V > v]}{P[U > u, V \leqslant v]P[U \leqslant u, V > v]} \tag{13}$$

where the numerator represents the product of probabilities when U and V are greater than or less than u and v simultaneously (possibility for positive dependence), and the denominator describes the product of probabilities when U and V have opposite trends (possibility for negative dependence). Therefore, U and V are positively dependent for $\psi_{UV} > 1$ (approaches $+\infty$ for perfectly positive dependence), negatively dependent for $\psi_{UV} < 1$ (approaches zero for perfectly negative dependence), and independent for $\psi_{UV} = 1$. For the Plackett family of distributions, this cross-product ratio is a constant. In terms of copula C_{UV}, Eq. (13) can be rewritten as

$$\psi_{UV} = \frac{C_{UV}(u,v)[1 - u - v + C_{UV}(u,v)]}{[u - C_{UV}(u,v)][v - C_{UV}(u,v)]} \tag{14}$$

Of the two possible solutions of Eq. (14), only the one with the negative sign before the radical provides an explicit expression for C_{UV} (Kao and Govindaraju, 2008):

$$C_{UV}(u,v) = \frac{[1 + (\psi_{UV} - 1)(u + v)] - \sqrt{[1 + (\psi_{UV} - 1)(u + v)]^2 - 4uv\psi_{UV}(\psi_{UV} - 1)}}{2(\psi_{UV} - 1)} \tag{15}$$

Parameter ψ_{UV} of the Plackett copula is related to Spearman's Rho Salvadori (2007) ($\rho s \neq 1$)

$$\rho s(\psi_{UV}) = \frac{\psi_{UV} + 1}{\psi_{UV} - 1} - \frac{2\psi_{UV}\log(\psi_{UV})}{(\psi_{UV} - 1)^2} \tag{16}$$

Thus, parameters of the Plackett copula can be estimated by Eq. (16).

3.5. Discordance test

The assessment of the discordancy measure of site i among a set of N sites is a first step before proceeding with homogeneity analysis. The discordancy test, proposed by Hosking and Wallis (1993, 1997), was extended to its multivariate framework by Chebana and Ouarda (2007). Assuming a matrix $U_i^t = \left[\Lambda_2^{*(i)}\Lambda_3^{*(i)}\Lambda_4^{*(i)}\right]$ for each site i, it contains these three matrices, i.e., $\Lambda_2^{*(i)}\Lambda_3^{*(i)}\Lambda_4^{*(i)}$ defined in Eqs. (6) and (7). Then the following matrix D_i is defined as:

$$D_i = \frac{1}{3}(U_i - \overline{U})' S^{-1}(U_i - \overline{U}) \tag{17}$$

where $S = (N-1)^{-1}\sum_{i=1}^{N}(U_i - \overline{U})(U_i - \overline{U})'$, $\overline{U} = N^{-1}\sum_{i=1}^{N}U_i$. In order to evaluate the discordancy of site i, it is possible to use a norm $||D_i||$ of the matrix D_i. This transformation from the multidimensional space to the real line has the advantage of defining an intuitive distance in the vector space and reducing exactly to the usual univariate case. There are several norms and the $||\cdot||_2$ norm is the most appropriate to properly quantify the variability (Chebana and Ouarda, 2007), and is defined as:

$$\|A\|_2 = \sqrt{\text{maximum eigenvalue of } \; A'A} \tag{18}$$

Constant $c = \chi 1 - 0.05(3)/3 = 2.6049$, where $\chi 1 - \alpha(d)$ is the quantile of a chi-square distribution of order a with d degrees of freedom, is suggested as a critical value for $||D_i||$ considered for large regions (Chebana and Ouarda, 2007). So, $||D_i|| > 2.6049$ indicates that site i is discordant in the region.

3.6. Homogeneity test

The logic of bivariate homogeneity is the same as that in the univariate homogeneity described by Hosking and Wallis (1993, 1997). Chebana and Ouarda (2007) described statistic $V_{\|\cdot\|}$ as:

$$V_{\|\cdot\|} = \left(\left(\sum_{i=1}^{N} n_i \right)^{-1} \sum_{i=1}^{N} n_i \left\| \Lambda_2^{*(i)} - \overline{\Lambda}_2^{*} \right\|^2 \right)^{1/2} \tag{19}$$

where $\|\cdot\|$ is the norm defined above, $\overline{\Lambda}_2^{*} = \left(\sum_{i=1}^{N} n_i\right)^{-1} \sum_{i=1}^{N} n_i \Lambda_2^{*(i)}$ and $\Lambda_2^{*(i)}$ defined in Eq. (7) is the L-covariance coefficient matrix for site i with a record length n_i, $i = 1,\ldots,N$. Similar to the univariate case, the observed value of statistic $V_{\|\cdot\|}$ is standardized using the mean and standard deviation values of $V_{\|\cdot\|}$ computed on the basis of a large number of simulated homogeneous regions. Hence the statistic that measures the heterogeneity of a set of sites is given by:

$$H_{\|\cdot\|} = \frac{V_{\|\cdot\|} - \mu_{Vsim}}{\sigma_{Vsim}} \tag{20}$$

where μ_{Vsim} and σ_{Vsim} are the mean and standard deviation of the N_{sim} values of $V_{\|.\|}$ of simulated regions. The simulated regions are homogeneous with sites having the same record lengths as their observed counterparts. To avoid any subjective choice of the bivariate distribution with which simulations are carried out to compute μ_{Vsim} and σ_{Vsim}, this bivariate distribution should be as general as possible and include most distributions commonly used in hydrology. Chebana and Ouarda (2007) used a Gumbel–Hougaard bivariate copula to produce the joint distribution and suggested to use a Kappa distribution to simulate the marginals. Meanwhile, the drought duration is fitted as exponential distribution if it is considered as a continuous random variable (Mathier et al., 1992; Shiau, 2006), and the gamma distribution is generally used to describe drought severity (Mathier et al., 1992; Shiau, 2006). To avoid the bias of distribution selection, the distributions for description of drought duration and severity were the exponential and gamma distributions, respectively, in the simulated regions. In this case, 1000 times simulations were done to validate the result. In this study, a region of sites was declared to be homogeneous if $H_{\|\cdot\|} < 1$, acceptably homogenous if $1 < H_{\|\cdot\|} < 2$ and definitely heterogonous if $H_{\|\cdot\|} > 2$.

3.7. Subjective adjustment

For a initial homogenous region clustered by the fuzzy *c*-means in this study, there may be still some sites discordant in the region, then subjective adjustments can often be necessary to improve the physical coherence of regions and to reduce the discordance of regions as measured by the discordance test (Rao and Srinivas, 2006; Yang et al., 2010). Several adjustments of regions were recommended (e.g. Hosking and Wallis, 1997): (1) move a site or a few sites from one region to another; (2) remove a site or a few sites from the dataset; (3) subdivide the region; (4) classify the target region by reassigning its sites to other regions; (5) merge the region with another or others; (6) merge two or more regions and redefine groups.

3.8. Copula estimation for homogenous regions

The marginal distributions of drought severity and duration were fitted using a procedure similar to the index flood proposed by Hosking and Wallis (1993), that is, for a homogeneous region the frequency distributions of the sites in the homogeneous region are identical, apart from a site-specific scaling factor. In this study, $\mu_{i,S}$ and $\mu_{i,D}$ denote the site-specific scaling factor for drought severity and duration, respectively.

Meanwhile for a homogeneous region identified by the multivariate homogeneity test, the bivariate joint distributions of the sites in the homogeneous region are assumed to be identical, and the observations from all of the sites in the homogeneous region are also with an identical marginal distributions, apart from a site-specific scaling factor, then in this study the bivariate copula of a homogeneous region was fitted using observations from all of the sites in the homogeneous region, noting that the observations have been standardized by the site-specific scaling factors. As the drought events in a site usually are not much enough, this method can improve the reliability of statistical estimates.

3.9. Frequency analysis

Let S denote drought severity and D drought duration. Drought events with long duration and (or) large severity may exercise a considerable influence on human society. In this case, the joint extreme events considered in this study are:

$$\{S > s\} \vee \{D > d\} \quad \text{and} \quad \{S > s\} \wedge \{D > d\}$$

where $\wedge$ denotes "and", and $\vee$ denotes "or". Then joint return periods related these two events were computed as:

$$T_{\{S>s \vee D>d\}} = \frac{\mu_t}{P(S > s \vee D > d)} = \frac{\mu_t}{1 - F(s,d)} \tag{21}$$

$$T_{\{S>s \wedge D>d\}} = \frac{\mu_t}{P(S > s \wedge D > d)} = \frac{\mu_t}{1 - F(s) - F(d) + F(s,d)} \tag{22}$$

where $F(s) = P(S \leqslant s)$, $F(d) = P(D \leqslant d)$, and $F(s, d)$ is the joint distribution; μ_t denotes the time interval, e.g., if the series studied is the annual maximum streamflow, then μ_t is 1 year. Based on the theory of runs and Markov theorem μ_t was computed as (Shiau and Shen, 2001):

$$\mu_t = \frac{1}{P_{DW}} + \frac{1}{P_{WD}} \tag{23}$$

wherein $p_{WD} = p(\mathrm{SPI}_t \leqslant -0.99|\mathrm{SPI}_{t-1} > -0.99)$ and $p_{DW} = p(\mathrm{SPI}_t > -0.99|\mathrm{SPI}_{t-1} \leqslant -0.99)$. Here, the unit of μ_t is month.

4. Results

4.1. Regionalization of droughts in the Pearl River basin

The topographical features of the Pearl River basin are complex, and the Pearl River basin is generally affected by southwest and southeast monsoon, the precipitation changes are far from being spatially homogeneous, so different climate patterns of annual monthly precipitation amounts were identified. In this case, the homogeneous regions were first differentiated by using the fuzzy *c*-means clusters in terms of the coefficient variation of monthly precipitation within a year. Generally, five homogeneous regions were identified based on the cluster validity index for the fuzzy *c*-mean proposed by Ramze Rezaee et al. (1998), and the results are not shown in the paper. The multivariate and univariate discordance test was done for each homogeneous region. Results (Table 2) of the initial cluster show that the discordance test based on the univariate variables of drought duration and severity indicated no sites discordant in each homogeneous region from initial cluster region. However as the multivariate discordance test could proper take account of the correlation between variables, it is found that station 26 was discordant in cluster I, stations 7 and 9 were discordant in cluster II and stations 12 and 25 were discordant in cluster III.

For these discordant stations, subjective adjustments can often be necessary to improve the physical coherence of regions and to reduce the heterogeneity of regions as measured by the heterogeneity

Table 2
Results of discordance tests for 42 meteorological gauges in the Pearl River basin from initial cluster, and the underline is selected as discordant in the initial cluster, *S* denotes the drought severity and *D* the drought duration, *DS* denotes the joint behavior of drought duration and severity.

Cluster I				Cluster II				Cluster III				Cluster IV				Cluster V			
Site	*D*	*S*	*DS*	Site	*D*	*S*	*DS*	Site	*D*	*S*	*DS*	Site	*D*	*S*	*DS*	Site	*D*	*S*	*DS*
2	1.49	0.97	1.51	1	0.76	0.04	0.15	12	1.63	1.56	5.56	23	0.66	1.32	0.82	37	1.00	1.00	1.37
3	0.65	0.87	0.40	6	1.57	1.04	0.65	13	2.70	2.42	0.89	24	0.22	0.58	0.14	41	1.00	1.00	0.09
4	1.45	1.30	2.40	7	0.57	1.81	2.80	14	1.48	1.45	1.32	31	0.61	0.60	1.32	42	1.00	1.00	1.22
5	1.02	2.22	0.67	8	0.45	0.23	0.73	17	0.40	0.26	0.34	32	2.11	1.71	0.74				
26	1.22	1.00	2.76	9	1.86	1.43	2.62	18	1.06	0.98	0.92	33	1.15	0.56	2.01				
27	0.70	0.52	1.31	10	1.06	1.15	0.63	19	1.40	1.70	0.37	34	0.78	0.81	2.44				
28	1.51	1.40	0.31	11	1.74	1.91	1.46	20	0.44	0.48	1.35	35	1.25	0.88	2.29				
38	0.50	0.68	1.23	15	0.21	0.80	0.41	21	0.74	0.53	1.08	36	1.94	1.81	0.68				
39	0.46	0.05	0.09	16	0.77	0.59	1.26	22	0.01	0.06	0.01	40	0.28	0.73	0.22				
								25	1.69	1.77	2.76								
								29	0.11	0.37	0.04								
								30	0.35	0.42	0.06								

Table 3
Results of discordance and homogeneity tests for the final adjusted homogeneous regions, *S* denotes the drought severity, *D* the drought duration and *DS* the joint behavior of drought duration and severity, discordancy measure critical value for univariate and bivariate cases are denoted by C_u and C_b, respectively.

	Site	Discordance test			Homogeneity test		
		D	*S*	*DS*	*D*	*S*	*DS*
Region I (C_u = 1.92, C_b = 2.60)	2	1.05	0.68	1.17	−0.89	−1.82	−1.67
	3	0.40	0.89	0.54			
	5	0.74	1.62	0.97			
	7	0.26	1.04	1.96			
	27	1.06	0.43	0.55			
	28	1.84	1.71	1.38			
	39	1.65	0.63	1.82			
Region II (C_u = 2.14, C_b = 2.60)	1	0.74	0.23	0.30	−0.12	−0.40	−1.14
	6	1.40	0.97	0.82			
	8	0.62	0.86	1.40			
	9	1.80	1.99	2.37			
	10	0.93	1.02	0.74			
	11	1.67	1.74	2.40			
	15	0.19	0.69	0.29			
	16	0.65	0.50	1.04			
Region III (C_u = 2.63, C_b = 2.60)	13	2.30	2.20	1.65	−0.34	−1.38	−1.45
	14	1.27	1.25	2.45			
	17	0.38	0.36	0.63			
	18	0.99	1.01	1.62			
	19	1.37	1.69	0.61			
	20	0.75	0.62	2.37			
	21	1.62	1.04	2.00			
	22	0.00	0.06	0.01			
	29	0.12	1.10	0.10			
	30	0.78	0.24	0.09			
	31	1.41	1.42	1.90			
Region IV (C_u = 1.92, C_b = 2.60)	23	0.44	1.11	0.87	−0.19	−1.06	−0.34
	24	0.76	0.65	1.18			
	25	0.33	0.67	0.17			
	32	1.64	1.33	2.46			
	35	1.40	1.51	2.53			
	36	1.29	0.85	0.38			
	40	1.14	0.86	0.47			
Region V (C_u = 1.33, C_b = 2.60)	33	1.31	0.57	1.22	−0.11	−0.40	−1.10
	34	1.19	0.84	1.65			
	37	0.24	1.29	0.06			
	41	0.93	1.00	0.74			
	42	1.32	1.29	1.66			

measure, and these can be done as illustrated in Section 3.7. After several adjustments, the final results of the identified homogeneous regions are illustrated in Table 3 and Fig. 4, which show that the entire Pear River basin can be categorized into five homogeneous regions. As stations 4, 12, 26 and 38 could not be grouped into any differentiated homogeneous region, they were excluded from the dataset. The homogeneity measure $H_{\|.\|}$ defined in Eq. (20) was calculated for the homogeneous regions detected and the results (Table 3) indicated that the homogeneous regions identified were corroborated statistically to be homogeneous with $H_{\|.\|} < 1$. And for univariate variables of drought severity and duration the homogeneous regions identified were also corroborated statistically to be homogeneous.

Boundaries of the each homogeneous region were demarcated by the following procedure: (1) the first step was to get the membership of any location belonging to each homogeneous region.

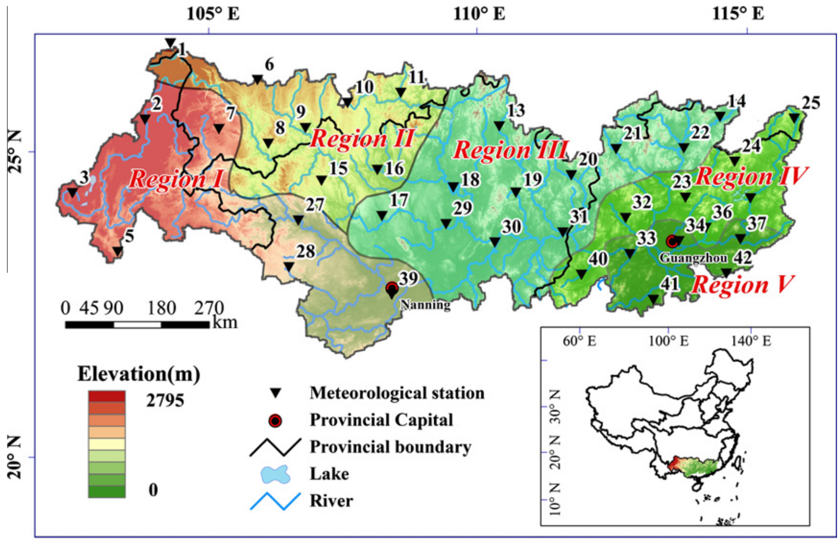

Fig. 4. Homogenous regions across the Pearl River basin.

Table 4
Goodness-of-fit test results of the regional fitted distribution for duration, severity and the joint behavior of drought duration and severity, and the underline is selected as the best regional fitted distribution.

	Duration			Severity			Copula (*p*-value)			
	PE3	GPA	EXP	PE3	GPA	GAM	Clayton	Frank	Gumbel	Plackett
Region I	2.15	3.98	−0.15	0.25	2.21	−2.27	0	0	0	0.010
Region II	3.09	4.71	1.34	1.26	3.08	−0.78	0	0	0	0.002
Region III	3.47	4.65	2.35	0.54	2.07	−1.23	0	0	0	0.022
Region IV	0.57	2.19	−1.32	−0.92	0.62	−2.90	0	0	0.001	0.071
Region V	2.74	3.69	1.72	1.15	2.52	−0.29	0	0	0	0.016

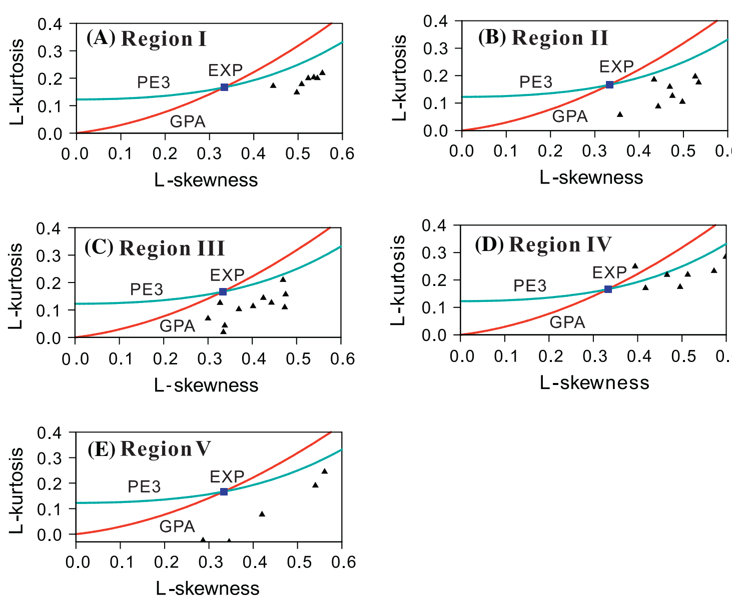

Fig. 5. L-moment ratio plot for drought duration at five homogeneous regions.

This was done by assigning 1 to the stations in any homogeneous region and 0 for other stations and interpolating them across the Pearl River basin by Inverse Distance Weighted (IDW) technique, respectively; (2) the second step was to get the membership of any location belonging to each homogeneous region. And the location was considered to be in the homogeneous region with the largest membership degree. Thus, whether a location was demarcated into a region was decided by the least spatial distance away from a homogeneous region in the Pearl River basin (Fig. 4).

4.2. Frequency analysis results

For each homogeneous region, the regional distribution of drought severity and duration was fitted by the General Pareto

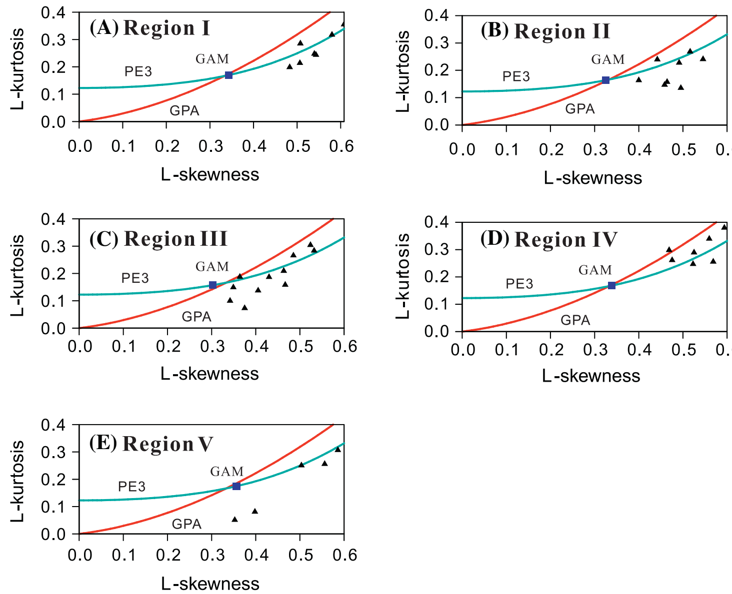

Fig. 6. L-moment ratio plot for drought severity at five homogeneous regions.

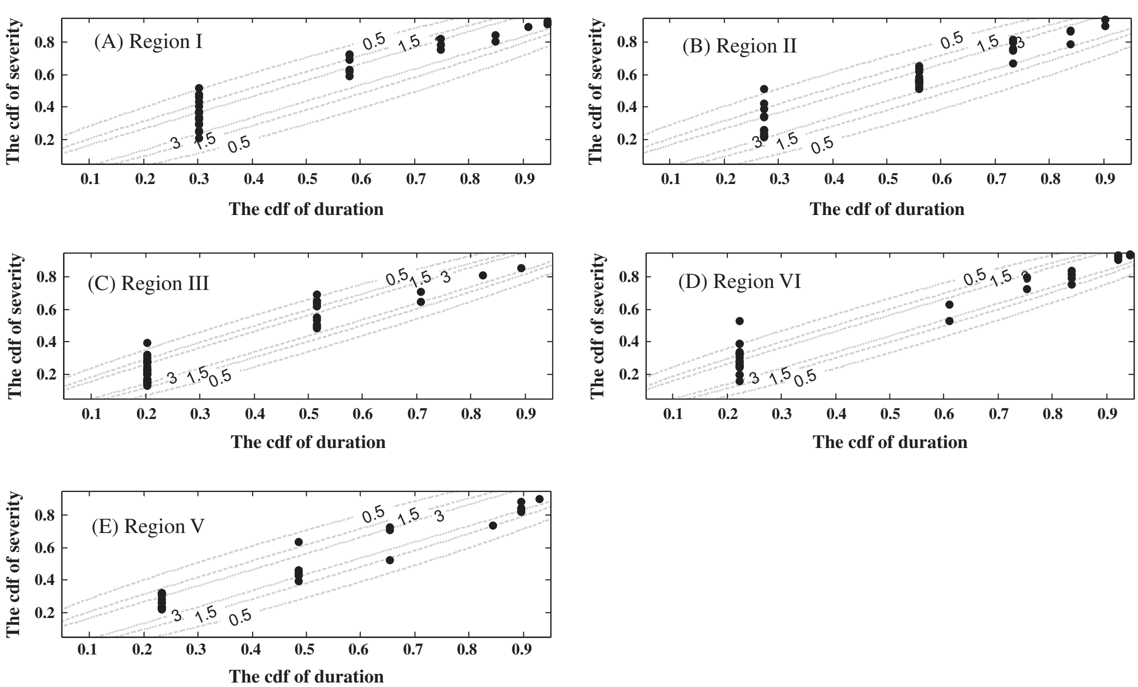

Fig. 7. The fitted Plackett copula for each homogeneous region, the contours denote the Plackett copula density and the dots denote the scatter plot of drought duration and severity based on the probability calculated by the regional fitted distributions.

distribution (GPA, 3 parameters); Pearson type III distribution (PE3, 3 parameters), Exponential Distribution (EXP, 2 parameters) and Gamma Distribution (GAM, 2 parameters), and the results are illustrated in Table 4, where the criterion value was 1.64 for the absolute value of goodness-of-fit measure statistic Z (Hosking and Wallis, 1997), corresponding to acceptance of the hypothesized distribution at a confidence level of 90%. If serial correlation or cross correlation is present in the data, such as the Pearson cross correlation of drought duration at stations 18 and 19 in region III is 0.2, being significant at 95% confidence level, the Z will be overestimated, Thus, a false indication of poor fit may be given. To overcome this problem, it is possible to generate simulated data that are correlated, but this is outside of the scope of this study, so the candidate distributions are not just determined by the criterion that the absolute value of Z less than 1.64. Furthermore, the L-moment ratio diagram is also used to identify the distribution by comparing its closeness to the L-skewness and L-kurtosis combination in the L-moment ratio diagram. The L-moment ratio plot for drought duration and severity at five homogeneous regions are illustrated in Figs. 5 and 6 respectively.

Based on the results of Table 4 and the L-moment ratio plots in Figs. 5 and 6, the best fit regional distributions of drought severity were PE3, PE3, PE3, PE3 and GAM for the homogeneous regions I to V, respectively. And the best fit regional distributions of drought

Table 5
Characteristic for each homogeneous region, and $\mu_{i,S}$, $\mu_{i,D}$ denote the site-specific scaling factor for drought severity and duration, respectively.

	Site	$\mu_{i,D}$	$\mu_{i,S}$	Drought episodes	Time interval (year)	Duration region fit distribution	Severity regional fit distribution	Regional best fit copula
Region I	2	2.14	3.33	36	1.25	EXP (xi = 0.13, alpha = 0.87)	PE3 (mu = 1, sigma = 1.22, gamma = 3.37)	Plackett (theta = 82.1)
	3	2.29	3.48	35	1.32			
	5	2.85	4.65	27	1.66			
	7	2.44	3.83	34	1.35			
	27	2.55	3.69	40	1.13			
	28	2.84	4.37	31	1.46			
	39	2.56	3.98	34	1.33			
Region II	1	2.33	3.57	36	1.25	EXP (xi = 0.15, alpha = 0.85)	PE3 (mu = 1, sigma = 1.10, gamma = 2.91)	Plackett (theta = 74.9)
	6	2.91	4.51	32	1.44			
	8	2.38	3.85	34	1.36			
	9	2.78	4.24	32	1.45			
	10	2.51	3.89	35	1.32			
	11	2.93	4.59	29	1.60			
	15	2.38	3.46	40	1.13			
	16	2.30	3.53	33	1.37			
Region III	13	2.33	3.44	40	1.13	EXP (xi = 0.22, alpha = 0.78)	PE3 (mu = 1, sigma = 1.00, gamma = 2.62)	Plackett (theta = 183.7)
	14	2.08	3.11	38	1.18			
	17	2.55	4.10	33	1.37			
	18	3.16	4.62	31	1.45			
	19	2.26	3.47	34	1.33			
	20	2.72	4.04	29	1.56			
	21	2.38	3.57	32	1.41			
	22	2.51	3.65	35	1.29			
	29	2.72	4.34	29	1.56			
	30	2.72	4.13	32	1.40			
	31	3.18	4.92	28	1.60			
Region IV	23	2.54	4.29	28	1.61	PE3 (mu = 1, sigma = 0.97, gamma = 3.04)	PE3 (mu = 1, sigma = 1.20, gamma = 3.30)	Plackett (theta = 159.9)
	24	2.78	4.48	27	1.67			
	25	2.85	4.42	27	1.67			
	32	2.36	3.42	36	1.25			
	35	2.23	3.36	35	1.29			
	36	3.03	4.70	29	1.55			
	40	2.47	3.53	34	1.32			
Region V	33	2.83	4.46	29	1.56	EXP (xi = 0.12, alpha = 0.88)	GAM (alpha = 0.87, kappa = 1.15)	Plackett (theta = 79.1)
	34	3.03	4.54	29	1.55			
	37	2.85	4.79	27	1.67			
	41	2.67	4.21	33	1.36			
	42	2.58	4.01	33	1.36			

duration were EXP, EXP, EXP, PE3 and EXP for the homogeneous regions I to V, respectively. Also it can be seen that the distributions fit for regional drought duration are not as good as for drought severity, this may be caused by the discreteness of duration (Fig. 7).

Goodness-of-fit tests for copulas based on Kendall's transform with the test statistic of the Cramér–von Mises functional S_n^K defined in Eq. (4) of Genest et al. (2009) were calculated for each homogeneous region, as shown in Table 4. It shows that, at the 99% confidence level, the null hypothesis can be accepted that the sample can follow a copula, the best fit copulas for the homogeneous regions except region II were the Plackett copula. However the p-value of goodness-of-fit tests for copulas based on Rosenblatt's transform with the test statistic of the Cramér–von Mises functional $S_n^{(B)}$ defined in Eq. (9) of Genest et al. (2009) is 0.01, being significant at 99% confidence level, then in this study the best fit copula for region II is also considered as the Plackett copula.

The estimation of the Plackett copula parameter was based on Spearman's Rho (Salvadori, 2007) as is illustrated in Section 3.4.3. Parameters of the regional fitted distributions of drought severity, drought duration and copula for each homogeneous region are illustrated in Table 5. Also illustrated in the table are the site-specific scaling factors of drought severity and duration, time interval and drought episodes. The density plots of Plackett copula for each homogeneous region have been illustrated in Figs. 7 and 8, and the scatter plot of drought duration and severity of a random station selected from each homogeneous region are also complemented (the stations were randomly selected from regions I to V are stations 27, 10, 19, 32, and 37 respectively). The scatter plot of drought duration and severity in Fig. 7 is based on the probability calculated by the regional fitted distributions. It can be seen that there are many ties for drought duration especially for short duration drought, and this may be attributed to the poor fit of copula and the marginal distribution of duration. However as the time series are limited, the detected drought episodes are not enough. Meanwhile, as the autocorrelation existed in the hydrological time series and the proper unit of SPI is month, which causes not proper detected drought durations. The ties of drought duration cannot be avoided, and then the multivariate regional frequency analysis method will help to improve the reliability of statistical estimates to a certain degrees if the drought is needed to be analyzed by multivariate variables.

The scatter plot of drought duration and severity in Fig. 8 is based on the probability of empirical cumulative distribution function, and the ties are ranked randomly. The goodness-of-fit tests for copula used in the paper are based on the empirical cumulative distribution, involving no parameter tuning or other strategic choices. It can be seen from Fig. 8 that the high probability parts of drought duration and severity are fitted well while the low probability parts are fitted less well.

As the regional copulas have been estimated, the frequency of drought properties can be analyzed. The joint return periods of

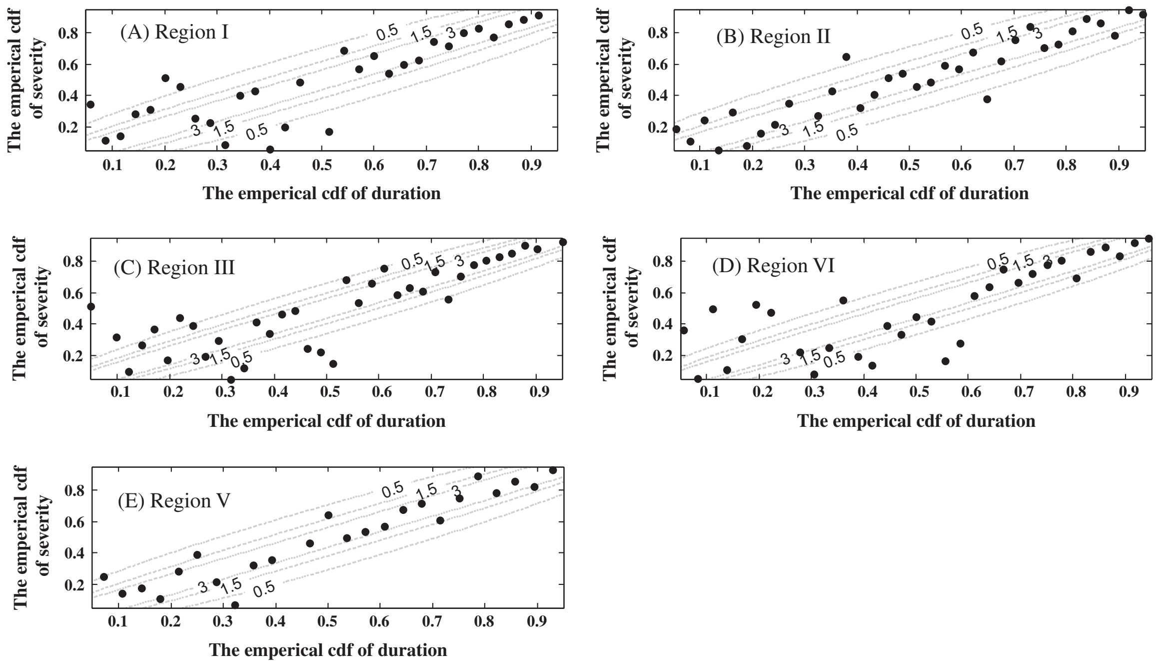

Fig. 8. The fitted Plackett copula for each homogeneous region, the contours denote the Plackett copula density and the dots denote the scatter plot of drought duration and severity based on the empirical cumulative distribution function.

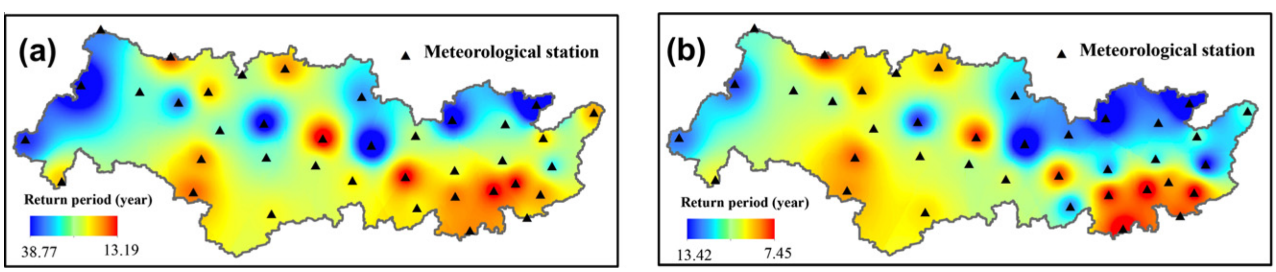

Fig. 9. Return period of drought duration as 6 months and drought severity defined by SPI as 7.5, (a) for the joint extreme drought event $\{S > s\} \wedge \{D > d\}$ and (b) for $\{S > s\} \vee \{D > d\}$.

drought severity large enough and (or) drought duration long enough were computed under two scenarios: (1) the drought duration was 6 months and the drought severity defined by SPI was 7.5, being considered as a moderate drought in this study; (2) the drought duration was 9 months and the drought severity defined by SPI was 11.25, being considered as a severe drought in this study. The results are illustrated in Figs. 9 and 10, respectively, being interpolated by Inverse Distance Weighted (IDW) technique.

Fig. 9a shows the spatial distribution of $T\{S > s \wedge D > d\}$ defined in Eq. (22) and Fig. 9b shows the spatial patterns of $T_{\{S>s \vee D>d\}}$ defined in Eq. (21). It can be observed from Fig. 9a that the average $T_{\{S>s \wedge D>d\}}$ characterized by the duration of 6 months and drought severity of 7.5 over the Pearl River basin was 21.18 years. Meanwhile a lower risk of droughts characterized by the duration of 6 months and drought severity of 7.5 can be found in the west and the northeast (around stations 19 and 21, refer to Fig. 1) parts of the Pearl River basin and a higher risk of drought in the Pearl River Delta. With average $T_{\{S>s \vee D>d\}}$ characterized by the duration of 6 months and drought severity of 7.5 over the Pearl River basin was 9.47 years, the spatial pattern of $T_{\{S>s \vee D>d\}}$ in Fig. 9b was similar to Fig. 9a, this means that higher risk of droughts of longer durations was always corresponding to the higher risk of droughts with severe drought severity, which poses an increasing challenge for drought management and water resources management.

The spatial distribution of return periods for the second scenario is shown in Fig. 10. Fig. 10a shows the spatial distribution of $T\{S > s \wedge D > d\}$ and Fig. 10b shows the spatial pattern of $T_{\{S>s \vee D>d\}}$. Similar features can be identified for the spatial distribution of return periods of droughts with longer durations and (or) higher severities, where average $T_{\{S>s \wedge D>d\}}$ and $T_{\{S>s \vee D>d\}}$ characterized by the duration of 9 months and drought severity of 11.25 over the Pearl River basin were 92.96 and 20.76 years, respectively. A lower drought risk can also be observed in the west and the northeast parts of the Pearl River basin and a higher risk of drought in the Pearl River Delta.

The Pearl River basin covers provinces of Yunnan, Guizhou, Guangxi, Guangdong, Hunan and Jiangxi, and the corresponding administrative divisions of the Pearl River basin are illustrated in Fig. 11. As most parts of the Pearl River basin are in Guangxi and Guangdong province, so in this paper, the information of historical drought in Guangxi and Guangdong provinces has been reviewed. Referring to Guangxi Meteorological Chi (Guangxi Zhuang Autonomous Region to the Local Records Commission, 1996), it is found that the agricultural drought in Guangxi occurs mainly in spring, and the risk of spring drought in Guangxi gradually reduced from southwest to the northeast of Guangxi. For example, the occurrence frequency of spring drought are highest in the Baise and lowest in the northeast Guilin area (the location of the area can be found in

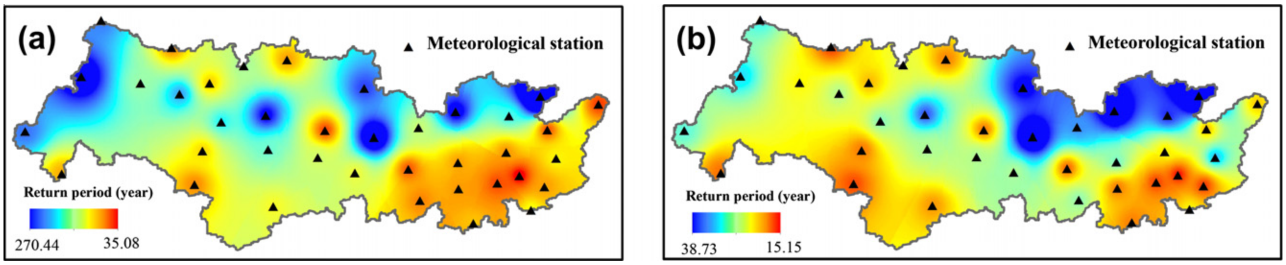

Fig. 10. Return period of drought duration as 9 months and drought severity defined by SPI as 11.25, (a) for the joint extreme drought event $\{S > s\} \wedge \{D > d\}$ and (b) for $\{S > s\} \vee \{D > d\}$.

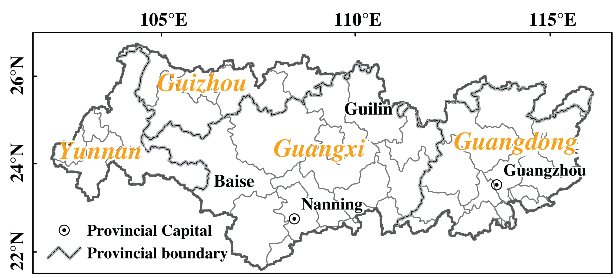

Fig. 11. Corresponding administrative divisions of the Pearl River basin.

Fig. 11), which is generally consistent with the results of Figs. 9 and 10. Referring to Guangdong Meteorological Chi (Guangdong Local Chronicles Compilation Committee, 1996). Besides, it is found that the spring drought is also dominant in Guangdong, and the risk of spring drought increases gradually from inland to coastal regions, i.e. from north to south of Guangdong (the location can be found in Fig. 11), being also generally consistent with the results of Figs. 9 and 10. Thus the results of this paper are of practical validity.

5. Conclusions

In frequency analysis of droughts, the absence of lengthy records usually limits the reliability of statistical estimates. To overcome this limitation, a multivariate regional frequency analysis approach is used in the Pearl River basin. Meanwhile, as the time series are limited, the detected drought episodes are not enough, and as the autocorrelation existed in the hydrological time series with the proper unit of SPI in month which may trigger not well-detected drought durations. There will be many ties of drought duration especially for the short drought duration. And this could be attributed to some poor fits of copula and the marginal distribution of duration.

The Pearl River basin can be categorized into five homogeneous regions in terms of drought variation. The copula goodness-of-fit test illustrates that Plackett copula fits well for all of the homogeneous regions. Under two predefined drought scenarios: (1) the drought duration is 6 months and the drought severity defined by SPI is 7.5; (2) the drought duration is 9 months and the drought severity defined by SPI is 11.25, the return period of a drought event with drought severity large enough and (or) drought duration long enough is calculated for all sites in each homogeneous region, and results show that the Pearl River Delta is characterized by a high drought risk, while a relatively lower drought risk in the west and northeast parts of the Pearl River basin. Results of this study will be helpful for basin-scale water resources management in the Pearl River basin, China.

Acknowledgments

The National Natural Science Foundation of China (Grant Nos. 41071020 and 50839005), Program for New Century Excellent Talents in University (NCET), a grant from the Research Grants Council of the Hong Kong Special Administrative Region, China (Project No. CUHK405308) and by the Geographical Modeling and Geocomputation Program under the Focused Investment Scheme (1902042) of The Chinese University of Hong Kong. Our cordial gratitudes should be extended to the editors, Prof. Dr. Andras Bardossy and Prof. Ercan Kahya, and two anonymous reviewers for their pertinent and professional comments and suggestions which are greatly helpful for further improvement of this manuscript.

References

Asquith, W.H., 2011. lmomco-L-moments, Trimmed L-moments, L-comoments, censored L-moments, and Many Distributions. R Package Version 1.3.6, Texas Tech University, Lubbock, Texas. <http://www.cran.r-project.org/package=lmomco>.
Cancelliere, A., Salas, D.J., 2010. Drought probabilities and return period for annual streamflows series. J. Hydrol. 391, 77–89.
Chebana, F., Ouarda, T., 2007. Multivariate L-moment homogeneity test. Water Resour. Res. 43 (8), W08406.
Dracup, J.A., Lee, K.S., Paulson Jr., E.G., 1980. On the definition of droughts. Water Resour. Res. 16 (2), 297–302.
Genest, C., Rémillard, B., Beaudoin, D., 2009. Goodness-of-fit tests for copulas: a review and a power study. Insurance: Math. Econom. 44 (2), 199–213.
Guangdong Local Chronicles Compilation Committee, 1996. Guangdong Province Chi: The Meteorological Chi. Guangdong People's Publishing House (in Chinese).
Guangxi Zhuang Autonomous Region to the Local Records Commission, 1996. Guangxi Gazetteer: The Meteorological Chi. Guangxi People's Publishing House (in Chinese).
Guttman, N.B., 1999. Accepting the standardized precipitation index: a calculation algorithm. J. Am. Water Resour. Assoc. 35 (2), 311–322.
Hosking, J.R.M., 1990. L-moments: analysis and estimation of distributions using linear combinations of order statistics. J. Roy. Stat. Soc. 52 (1), 105–124.
Hosking, J., Wallis, J., 1993. Some statistics useful in regional frequency analysis. Water Resour. Res. 29 (2), 271–281.
Hosking, J., Wallis, J., 1997. Regional Frequency Analysis: An Approach Based on L-moments. Cambridge Univ. Pr.
Kao, S.C., Govindaraju, R., 2008. Trivariate statistical analysis of extreme rainfall events via the Plackett family of copulas. Water Resour. Res. 44, W02415.
Kao, S.-C., Govindaraju, R.S., 2010. A copula-based joint deficit index for droughts. J. Hydrol. 380, 121–134.
Lei, Y.H., Duan, A.M., 2011. Prolonged dry episodes and drought over China. Int. J. Climatol. 31 (12), 1831–1840.
Liu, C.-L., Zhang, Q., Singh, P.V., Cui, Y., 2011. Copula-based evaluations of drought variations in Guangdong, south China. Nat. Hazards 59 (3), 1533–1546.
Livada, I., Assimakopoulos, V.D., 2007. Spatial and temporal analysis of drought in Greece using the standardized precipitation index (SPI). Theoret. Appl. Climatol. 89, 143–153.
Lloyd-Hughes, B., 2012. A spatio-temporal structure-based approach to drought characterisation. Int. J. Climatol. http://dx.doi.org/10.1002/joc.2280.
Mathier, L., Perreault, L., Bobë, B., Ashkar, F., 1992. The use of geometric and gamma-related distributions for frequency analysis of water deficit. Stochastic Hydrol. Hydraul. 6 (4), 239–254.
McKee, T.B., Doesken, N.J., Kleist, J., 1993. The relationship of drought frequency and duration to time scales. Preprints Eighth Conference on Applied Climatology, American Meteorological Society, Anaheim, CA, pp. 179-184.
Mishra, K.A., Singh, P.V., 2010. A review of drought concepts. J. Hydrol. 391, 202–216.
Nelsen, R.B., 2006. An Introduction to Copulas. Springer Verlag.
Plackett, R.L., 1965. A class of bivariate distributions. J. Am. Stat. Assoc. 60 (310), 516–522.
Rao, A.R., Srinivas, V.V., 2006. Regionalization of watersheds by fuzzy cluster analysis. J. Hydrol. 318, 57–79.
Renard, B., Lang, M., 2007. Use of a Gaussian copula for multivariate extreme value analysis: some case studies in hydrology. Adv. Water Resour. 30 (4), 897–912.

Ramze Rezaee, M., Lelieveldt, B.P.F., Reiber, J.H.C., 1998. A new cluster validity index for the fuzzy *c*-mean. Pattern Recogn. Lett. 19 (3–4), 237–246.
Salvadori, G., 2007. Extremes in Nature: An Approach Using Copulas. Springer Verlag.
Serfling, R., Xiao, P., 2007. A contribution to multivariate L-moments: L-comoment matrices. J. Multivar. Anal. 98 (9), 1765–1781.
Shiau, J.T., Shen, H.W., 2001. Recurrence analysis of hydrologic droughts of differing severity. J. Water Resour. Plann. Manage. 127 (1), 30–40.
Shiau, J., 2006. Fitting drought duration and severity with two-dimensional copulas. Water Resour. Manage 20 (5), 795–815.
Sklar, A., 1959. Fonctions de répartition àn dimensions et leurs marges. Publ. Inst. Statist. Univ. Paris 8, 229–231.
Vörösmarty, J.C., Green, P., Salisbury, J., Lammers, B.R., 2000. Global water resources: vulnerability from climate change and population growth. Science 289, 284–288.
Wilhite, D.A., 2000. Drought as a natural hazard: concepts and definitions. In: Wilhite, D.A. (Ed.), Drought: A Global Assessment. Routledge, London and New York, 3–18pp.
Wilhite, D.A., Glantz, M.H., 1985. Understanding the drought phenomenon: the role of definitions. Water Int. 10 (3), 111–120.
Wong, S.J., Zhang, Q., Chen, Y.D., 2010. Statistical modeling of daily urban water consumption in Hong Kong: trend, changing patterns, and forecast. Water Resour. Res. 46, W03506. http://dx.doi.org/10.1029/2009WR008147.
Yang, T., Shao, Q., Hao, Z.C., Chen, X., Zhang, Z., Xu, C.-Y., Sun, L., 2010. Regional frequency analysis and spatio-temporal pattern characterization of rainfall extremes in the Pearl River basin, China. J. Hydrol. 380 (3–4), 386–405.
Yevjevich, V., 1967. Objective Approach to Definitions and Investigations of Continental Hydrologic Droughts. Hydrology Paper 23, Colorado State U, Fort Collins, August 1967, 19 p, 9 fig, 1 tab, 12 ref.
Zhang, Q., Xu, C.-Y., Zhang, Z., 2009a. Observed changes of drought/wetness episodes in the Pearl River basin, China, using the standardized precipitation index and aridity index. Theoret. Appl. Climatol. 98, 89–99.
Zhang, Q., Xu, C.-Y., Gemmer, M., Chen, Y.D., Liu, C., 2009b. Changing properties of precipitation concentration in the Pearl River basin, China. Stoch. Env. Res. Risk Assess. 23 (3), 377–385.
Zhang, Q., Chen, Y.D., Chen, X., Li, J., 2011. Copula-based analysis of hydrological extremes and implications of hydrological behaviors in the Pearl River basin, China. J. Hydrol. Eng. 16 (7), 598–607.
Zou, X., Zhai, P.M., Zhang, Q., 2005. Variations in droughts over China: 1951–2003. Geophys. Res. Lett. 32, L04707. http://dx.doi.org/10.1029/2004GL021853.
Zhang, L., Singh, V.P., 2006. Bivariate flood frequency analysis using the copula method. J. Hydrol. Eng. 11, 150–164.
Zhang, L., Singh, V.P., 2007. Bivariate rainfall frequency distributions using Archimedean copulas. J. Hydrol. 332, 93–109.